Supplemental Figures

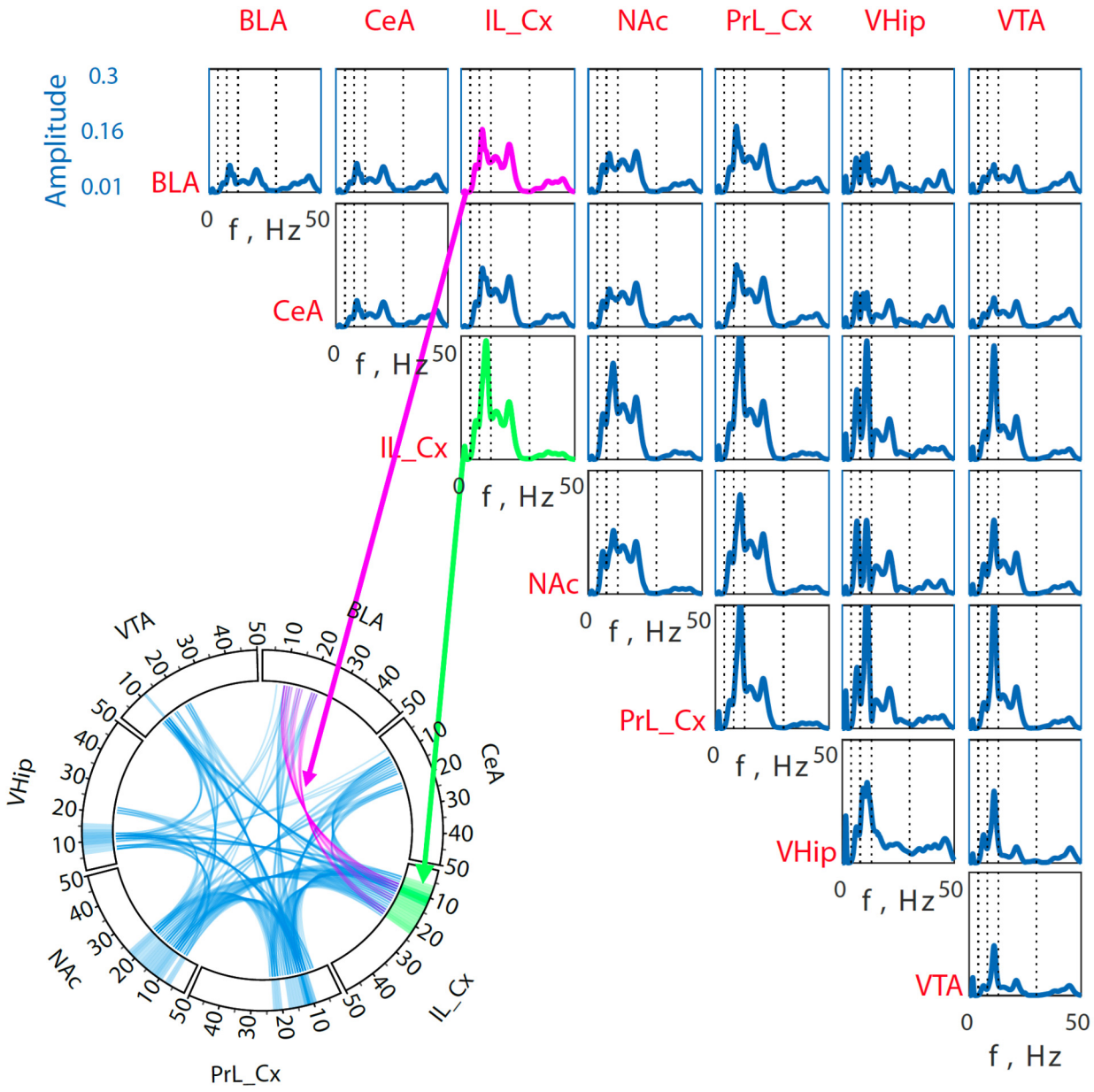

Supplemental Figure S1: Example of autocorrelation and cross-correlation functions that define an *Electome*. Brain areas are shown to the top and the left identifying auto-correlation and cross-correlation density functions for *Electome* 1. The circular plot is depicted at an amplitude threshold of 0.08.

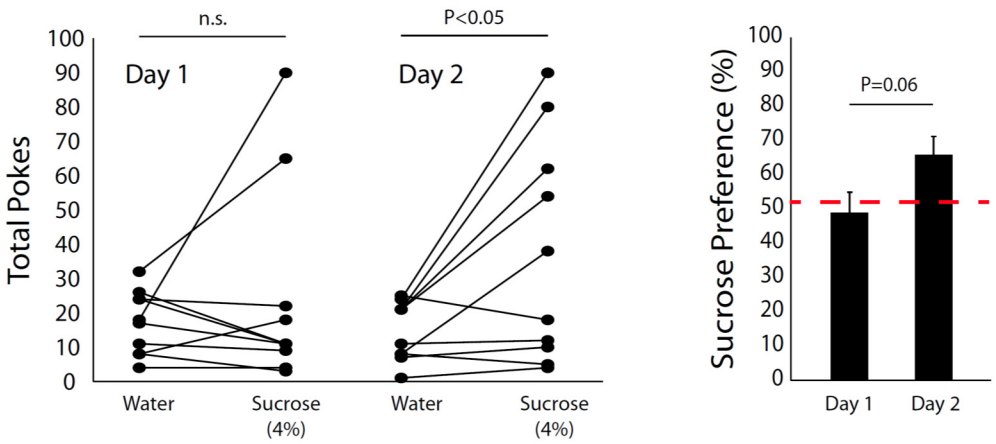

Supplemental Figure S2: Establishment of sucrose preference assay in C57 mice. C57 mice were placed in the testing chamber for one hour on two consecutive days. Preference for sucrose was observed across the population on the second, but not first testing day (t_9=0.86 and P=0.41; t_9= 2.7 and P=0.026 for Day 1 and Day 2, respectively, using two-tailed paired t-test. N=10 mice).

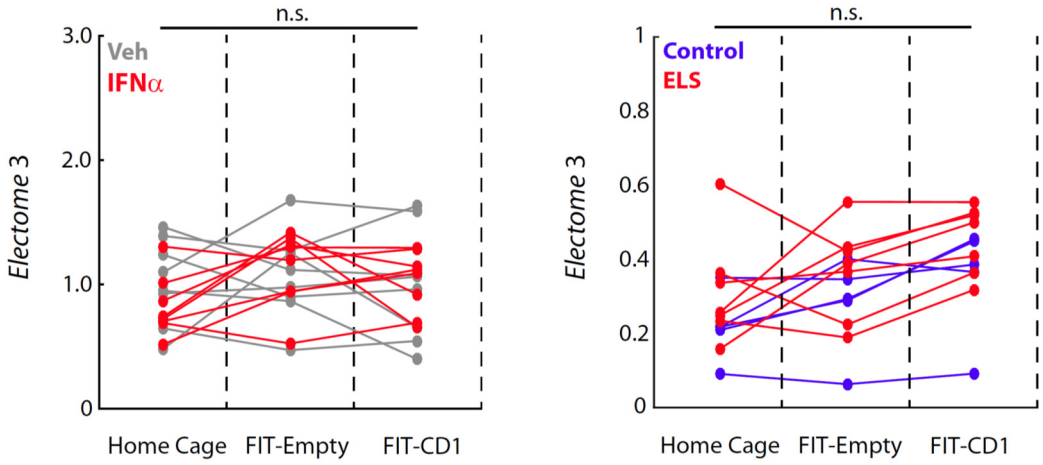

Supplemental Figure S3: *Electome 3* activity tends to be increased in one translational model of MDD vulnerability. Treatment with IFNα failed to increase *Electome 3* activity ($F_{1,28}$=0.05, P=0.41 for group effect). Early life stress tended to increase *Electome 3* activity, though these differences did not reach statistical significance ($F_{1,20}$=2.8, P=0.06 for group effect).

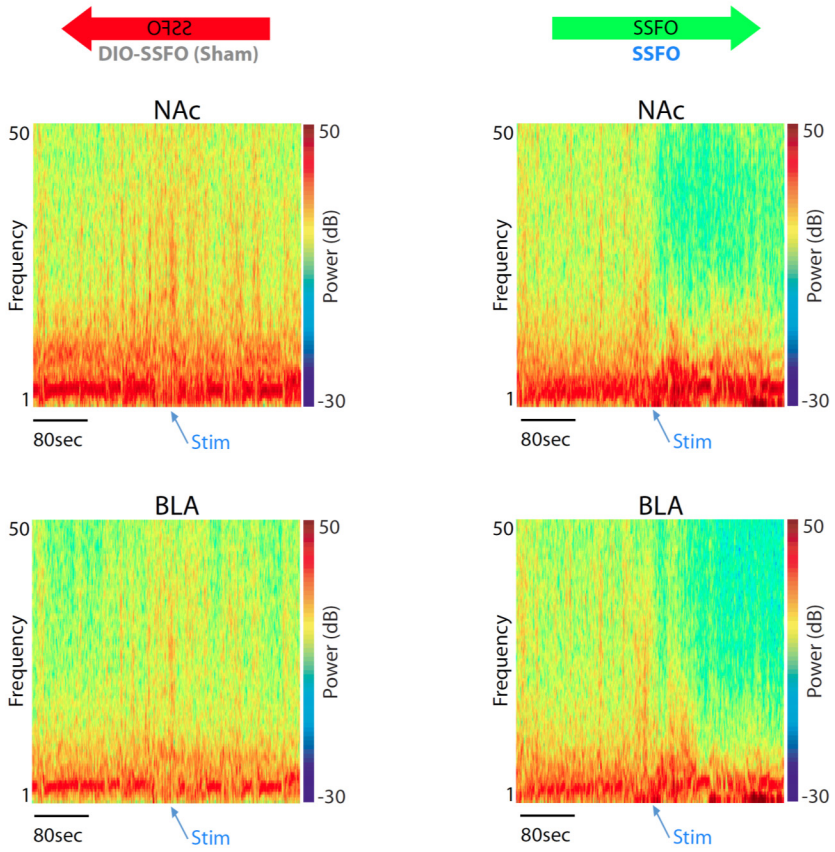

Supplemental Figure S4: Spectral plots showing LFP activity in NAc and BLA prior to and following IL_Cx light stimulation. Our IL_Cx-DBS protocol suppressed *Electome 2* activity. The suppression did not solely reflect stimulation induced changes in local IL_Cx oscillatory activity.

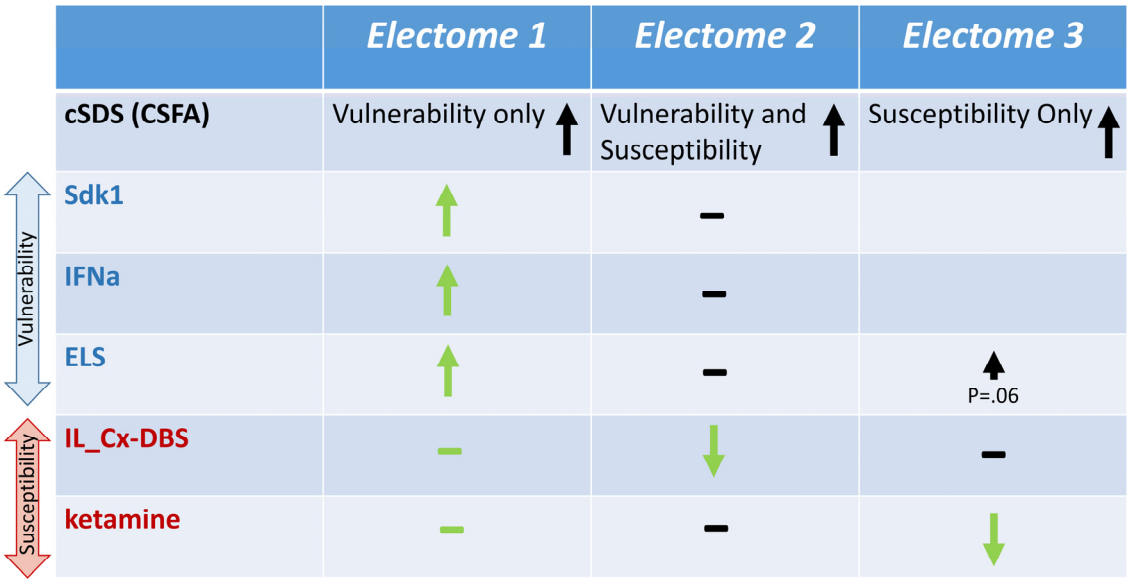

Supplemental Figure S5: Impact of experimental manipulations on *Electome* activity. Our data driven CSFA model raised the hypotheses that higher *Electome 2 and 3* activity signal the stress-susceptible syndrome that occurs after cSDS. What is more, our model raised the hypotheses that higher *Electome 1 and 2* activities signal which stress-naïve mice will exhibit the behavioral deficits that define stress-susceptibly after cSDS (innate vulnerability). We performed validation experiments for the two putative vulnerability signatures using three independent MDD-vulnerability models (Sdk1, IFNα, and ELS). All three experiments confirmed that increased *Electome 1* activity signaled MDD-vulnerability. These results are highlighted in green. All three experimental manipulations failed to validate Electome 2 activity as a signal of MDD-vulnerability. These negative results are highlighted in black. Next, we tested whether antidepressant-like manipulations that have been shown previously to target susceptibility would suppress the *validated Electome 1* vulnerability signature. We hypothesized that they would not, as would be the case if vulnerability and susceptibility are the result of distinct biological mechanisms. IL_Cx-DBS and ketamine failed to suppress *Electome 1* activity, confirming our hypothesis (highlighted by green). Ketamine failed to suppress *Electome 1* activity as well.

Our experimental approach also yielded incidental validation testing for the *Electomes* that signaled susceptibility in the cSDS model. *Electome 2* activity was suppressed by IL_Cx-DBS, but not ketamine. *Electome 3* activity was suppressed by ketamine, but not IL_Cx-DBS. Finally, we found that ELS also tended to increase *Electome 3* activity, though this change did not reach statistical significance (highlighted by small pink arrow; **P=0.06).

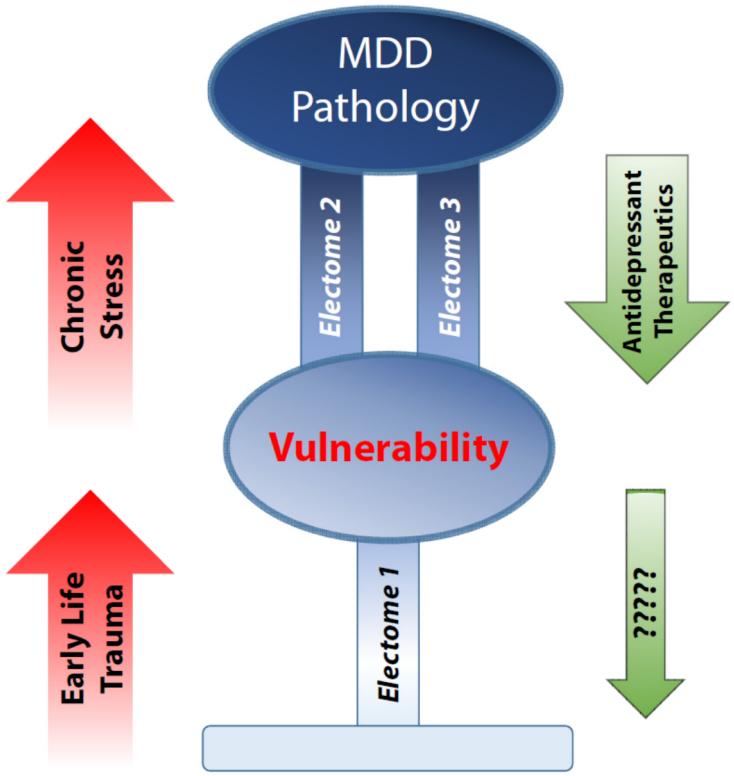

Supplemental Figure S6: Putative model of MDD vulnerability and behavioral dysfunction based on experimental observations. Experiences such as early life trauma increase *Electome 1* activity which promotes vulnerability. Chronic stress in vulnerable animals increases *Electome 2 and 3* activity, yielding MDD pathology. Antidepressants suppress *Electome 2 and 3* to reverse behavioral pathology. Manipulations that suppress *Electome 1* in stress-naïve mice remain to be discovered.

Supplemental Methods

Electrode Implantation Surgery

Mice were anesthetized with 1.5% isoflurane, placed in a stereotaxic device, and metal ground screws were secured above the cerebellum and anterior cranium. The recording bundles designed to target amygdala (AMY), NAc, VTA, PFC, and VHip were centered based on stereotaxic coordinates measured from bregma (AMY: -1.6mm AP, 2.75 mm ML, -3.9 mm DV from the dura; NAc: 1.6mm AP, 1.4mm ML, -3.5 mm DV from the dura; PFC: 1.7mm AP, 0mm ML, 2.25mm DV from the dura; VTA: -3.3mm AP, 0.5 mm ML, -4.25 mm DV from the dura; (VHip: -3.7mm AP, 3.0mm ML, -3.5mm DV from the dura). We chose these coordinates to match the coordinates utilized in our prior molecular studies in the cSDS model[1]. We targeted PrL and IL using the PFC bundle by building a 0.5mm DV stagger into our electrode bundle. Similarly, we targeted BLA and CeA by building a 0.5mm ML stagger and 0.3mm DV stagger into our AMY electrode bundle[2]. Histological analysis of implantation sites was performed at the conclusion of experiments to confirm recording sites used for neurophysiological analysis[2].

Homecage Recordings

Mice were connected to a headstage (Blackrock Microsystems, UT, USA) without anesthesia, and placed a new home cage. Recording were initiated after a 30 minute habituation period.

Forced Interaction test

The forced interaction test was performed as previously described[2, 3]. Notably, a homecage recording was always performed immediately prior to the start of the forced interaction test. C57 mice were placed in a 3.25” x 7” Plexiglas cylinder. Following a five minute recording period during which neurophysiological activity was recorded, a CD1 aggressor mouse was introduced to the cage outside of the cylinder (18” high walls surround the outer cage to prevent escape and a lid is place over the inner chamber to prevent the aggressor from climbing in). Neurophysiological data were then recorded for five additional minutes. Mice used to build the *Electome* model were subjected to the forced interaction test prior to and after exposure to cSDS. Mice used for the Sdk1 overexpression experiment were subjected to the forced interaction test prior to and after viral infection. Mice used for the IFNα and maternal separation stress experiments were only subjected to the forced interaction test once in adulthood.

Chronic social defeat stress

Mice implanted with electrodes underwent 10 days of cSDS as previously described[2, 4, 5]. Specifically, male retired-breeder CD1 (Charles River) mice were used as resident aggressors for the social defeat and were singly-housed prior to the experiments. Particularly aggressive CD1s, as defined by demonstrating at least one successful act of aggression toward an intruder C57 male within 60 sec, were selected for use. C57 mice were singly housed prior to undergoing social defeat. Intruder male C57 mice were introduced to the cage of a novel CD1 aggressor for 5 min daily, and then housed adjacent to the same aggressor for 24 hours. During this time, mice were separated by a transparent and porous plexiglass barrier to enable constant sensory exposure. During bouts of exposure to the CD1 mice, hallmark behavioral signs of subordination stress were observed including escape, submissive postures (i.e., defensive upright and supine) and freezing. Following the last 24 hr exposure to a CD1 aggressor mouse, all C57s were housed individually. Mice that exhibited significant injuries during social defeat stress were removed from post-stress analysis[2]. Several animals used to construct the initial cSDS *Electome* model were also used in our prior study[2]. Neither the pre-stress data presented in this study nor any neurophysiological activity from VHip were used for any prior analysis.

Choice social interaction test

Mice were placed within a novel arena (46cm x 46cm) with a small cage located at one end, and each mouse's movement was monitored for 150 seconds. Mice were then removed from the testing chamber, and reintroduced 30 seconds later after a non-aggressive CD1 mouse was placed in the small cage. The time C57 mice spent in the interaction zone was quantified using Ethovision XT 7.1 software (Noldus Information Technology, Wageningen, Netherlands). The interaction ratio was calculated as (Interaction time when CD1 was present)/(Interaction time when CD1 was absent)[2, 3, 6].

Cross-Spectral Factor Analysis (CSFA)

We used a latent factor analysis model, where individual factors were modeled as draws from Gaussian processes, to capture brain spatiotemporal dynamics features in an integrated brain-wide construct. Gaussian processes are non-parametric probabilistic descriptions of data that offer a powerful basis for non-linear multivariate regression and classification tasks, and are widely utilized in the machine learning literature. The probabilistic relations between data are determined by the Gaussian process "kernels" that describe covariance. We recently designed a novel Gaussian process kernel termed the Cross-Spectral Mixture kernel, which allows for the discovery of LFP features that incorporate spectral power, synchrony and phase-directionality between many brain regions[7]. A factor defined by the Cross-Spectral Mixture kernel is denoted as an *Electome*. We used such cross-spectral mixture kernels within a multiple-kernel-learning framework[8] where the measured LFP signals are represented as a linear combination of these GP latent functions. By windowing the data, we track the expressed strength of these factors over time. Briefly, each time-window includes N observations from R distinct brain regions. N is determined by the sampling rate and the length of time that each window represents. We represent the matrix of observations from window w by $\boldsymbol{Y}^w = [\boldsymbol{y}_1^w, \dots, \boldsymbol{y}_N^w] \in \mathbb{R}^{R\times N}$. These observations are located on a temporal grid, such that each $\boldsymbol{y}_n^w$ corresponds to the relative time location x_n^w within the window and the difference between subsequent samples is given by $x_n^w - x_{n-1}^w \triangleq \delta$ where $1/\delta$ represents the sampling rate of the LFP time-series. We model each temporal observation in a window by

$$\boldsymbol{y}_n^w = \boldsymbol{f}_w(x_n^w) + \boldsymbol{\epsilon}_n^w,$$

where $\boldsymbol{\epsilon}_n^w \sim N(\boldsymbol{0}, \gamma^{-1}\boldsymbol{I})$ is additive Gaussian noise with precision γ, and the latent function $\boldsymbol{f}_w(x_n^w)$ at time location x_n^w is the underlying process generating $\boldsymbol{y}_n^w$. The factor for the complete window is denoted as $\boldsymbol{F}_w(\boldsymbol{x}^w) = [\boldsymbol{f}_w(x_n^w), \dots, \boldsymbol{f}_w(x_n^w)] \in \mathbb{R}^{R\times N}$

A latent factor model is constructed according to

$$\boldsymbol{F}_w(\boldsymbol{x}) = \sum_{\ell=1}^{L} s_{w\ell}\boldsymbol{F}_w^\ell(\boldsymbol{x}),$$

where a linear combination of L latent factors, given by the functions $\{\boldsymbol{F}_w^\ell(\boldsymbol{x})\}_{\ell=1}^L$, represents $\boldsymbol{F}_w(\boldsymbol{x})$ [9]. The parameters $\boldsymbol{s}_w = [s_{w1}, \dots, s_{wL}]^T$ are a vector of factor scores, and are unique to each time window. The factor scores denote how strongly each *Electome* is expressed.

Importantly, every window independently draws the l^{th} latent functions from an identical distribution. In this way, the factors are not directly shared across time windows; rather, the underlying cross-spectral content (power and phase synchrony) of the signals is shared. To obtain this effect, a prior distribution is placed over the latent functions that encodes the full cross-spectrum, given by the multi-output Gaussian process[10, 11].

$$\boldsymbol{F}_w^\ell(x) \sim \mathcal{GP}\big(\boldsymbol{0}, \boldsymbol{K}_{\text{CSM}}(\boldsymbol{x}, \boldsymbol{x}'; \boldsymbol{\theta}_\ell)\big),$$

where the covariance kernel $\boldsymbol{K}_{\text{CSM}}(x, x'; \boldsymbol{\theta}_\ell)$ establishes the dependency structure between all latent function values $\boldsymbol{F}_w^\ell = [\boldsymbol{f}_w^\ell(x_n^w), \dots, \boldsymbol{f}_w^\ell(x_n^w)]$ is described by the cross-spectral mixture kernel. That is, $(\boldsymbol{K}_{\text{CSM}}(x, x'; \boldsymbol{\theta}_\ell))_{ij} \triangleq \text{cov}(f_{wi}^\ell(x), f_{wj}^\ell(x'))$ defines, within window w, how the observation at time x in region i covaries with the observation at time x' in region j. Each factor is provided a unique set of parameters $\boldsymbol{\theta}_\ell$, which contain the kernel parameters defining a stationary, multi-output cross-spectral mixture (CSM) kernel[7]. The CSM kernel represents the cross-spectra between the R regions as the real part of a complex mixture of Gaussians[7, 12]. For identifiability in the factor model, the CSM kernels are restricted to a correlation function such that $\max\left(\text{diag}\left(\boldsymbol{K}_{\text{CSM}}(0,0; \boldsymbol{\theta}_\ell)\right)\right) = 1$ for all ℓ.

During inference, all latent functions are marginalized out and gradient-based optimization is typically used to obtain the set of parameters $\boldsymbol{\Theta} = \{\{\boldsymbol{\theta}_\ell\}_{\ell=1}^L, \{\boldsymbol{s}_w\}_{w=1}^W, \gamma\}$ that maximize the log marginal likelihood, $\ln p(\boldsymbol{Y}|\boldsymbol{\Theta})$[11]. We provide a slight modification to directly maximizing the marginal likelihood. In this latent factor setting, one may desire the factors to both uncover data-fitting latent structure and inherit strong predictive power pertaining to recorded side information (e.g., task condition or whether an animal was subject to chronic social defeat stress). A supervised max-margin formulation[13] allows the factor scores $\boldsymbol{s}_w$ to be predictive of this side information, thereby encouraging the model to extract latent features relevant to the electrophysiological signatures of these conditions.

Each window is provided a class label $z_w \in \{-1,1\}$. Denoting $\boldsymbol{a} \circ \boldsymbol{b}$ as the elementwise vector product, we desire the factor scores $\tilde{\boldsymbol{s}}_w = \boldsymbol{s}_w \circ \boldsymbol{s}_w \in \mathbb{R}^L$ to be predictive of the class label z_w for each window w. Max-margin optimization problems attempt to find the optimal hyperplane that separates the two classes[14]. In particular, classification parameters $\boldsymbol{\Psi}$ are introduced, and a linear discriminant function is defined by $g(\tilde{\boldsymbol{s}}_w; \boldsymbol{\Psi}) = \boldsymbol{\beta}^T \tilde{\boldsymbol{s}}_w + b$, with $\boldsymbol{\Psi} = \{\boldsymbol{\beta}, b\}$. The classification rule $\hat{z}_w = \text{sign}(g(\tilde{\boldsymbol{s}}_w; \boldsymbol{\Psi}))$ is used to form a prediction of the class label. The optimization problem

$$\underset{\boldsymbol{\Theta}, \boldsymbol{\Psi}}{\arg\min} \sum_{w=1}^{W} -\log p(\boldsymbol{Y}^w|\boldsymbol{\Theta}) + \frac{1}{2}||\boldsymbol{\beta}||^2$$

$$\text{s.t.} \qquad z_w g\left(\tilde{\boldsymbol{s}}_w; \boldsymbol{\Psi}\right) \geq 1 \qquad \forall w$$

enforces maximum separability between classes by satisfying the hinge loss function $(1 - z_w g(\tilde{\boldsymbol{s}}_w; \boldsymbol{\Psi}))_+ = 0$ for all windows, where $(x)_+ = \max(0, x)$. An ℓ_2-regularization penalty is placed on $\boldsymbol{\beta}$ for identifiability. Because examples are not perfectly separable by a hyperplane, max-margin slack variables are introduced during inference. An alternating minimization strategy is used to alternate between updating data-fit parameters $\boldsymbol{\Theta}$ and classification parameters $\boldsymbol{\Psi}$. See appendix for further details.

We note a few unique aspects of this approach. 1) While prediction is often performed in a downstream processing component (e.g., first fit a latent factor model, then train an SVM independently on the factor scores), the ability to *jointly* infer model parameters with a max-margin model improves predictive power while simultaneously uncovering latent structure[13]. 2) As discussed, the optimization of classification parameters $\boldsymbol{\Psi}$ amounts to solving a max-margin classifier (e.g., the well-studied support vector machine) as a sub-problem, allowing the exploitation of pre-existing implementations in many standard software packages. 3) The factor scores in the Gaussian process factor model are a non-linear

embedding of the multi-channel time-series observations; this embedding is analogous to a non-linear version of supervised dictionary learning[15] and to interpretable descriptive neural networks[16] with imposed structure on cross-spectral density estimation.

We used a total of 44 C57 mice for our CSFA analysis. We used 19 mice subjected to cSDS and 16 non-stressed controls in the post-stress data. All 35 of these mice were also used in the pre-stress data group. Data from 9 additional mice were included in the pre-stress, but not post-stress, data set. Adding these 9 mice assured that the predictive factors learned for the home cage—forced interaction test segments did not contain mouse specific signals that yielded incidental putative vulnerability signatures in the pre-stress data set.

Hyper-parameter selection

Our objective was to learn four predictive features (±chronic stress, susceptibility/resilience, part 1 of forced interaction test, part 2 of forced interaction test). To our initial descriptive factor, we added 4 predictive factors and a 50% increase in factor number to allow for model flexibility. To our initial descriptive factor, we added 4 predictive factors and a 50% increase to allow for model flexibility. This resulted in 6 predictive factors. Our analysis included in 35 mice in the post-stress (non-stressed controls plus stress-mice) group. In order to avoid our descriptive factorings learning individual mice, we added 1 additional factor for every two mice in our supervised set of 35 mice. This resulted in 18 additional factors for a total of 25. All of the factors were descriptive of the local field potential signals, but predictions were only limited to the six factors to force a compact, scientifically testable hypothesis space.

Spike-*Electome* activity correlation

Data acquired during the 'post-stress' forced interaction test were used for this analysis. Unit firing activity was averaged within 5 second non-overlapping windows for the 20 minute recording period (10 minutes home cage, 10 minutes forced interaction test). A Rho_{Raw} was calculated for each spike and *Electome* correlation using the spearman rank test. We then randomly shuffled the bins of spike activity within the homecage and each segment of the forced interaction test, and recalculated the spearman rank to yield a Rho_{Rand}. We repeated this shuffling procedure 10,000 times to yield a distribution of correlation values expected by chance between each unit and *Electome* and ranked the resulting Rho_{Rand} values. The *Electome* coefficient score for a unit was then defined as Rho_{Raw}-$\Sigma(Rho_{Rand})/10{,}000$. *Electome*-Spike coefficient was considered significant for Rho_{Raw} values less than the 62^{nd} lowest Rho_{Rand} or higher than the $9{,}937^{th}$ highest Rho_{Rand} value of the chance distribution (corresponding to an $\alpha=0.05$ with Bonferroni correction for the 4 *Electomes* tested).

Sdk1 viral surgery for accelerated defeat

Mice were anaesthetized with ketamine (100mg/kg) and xylazine (10mg/kg) and placed in a small-animal stereotaxic instrument (Kopf Instruments). HSV virus (0.5uL of either HSV-Sdk1 or HSV-GFP) was bilaterally infused using 33-gauge syringe needles (Hamilton) into the vHIP (bregma coordinates: anterior/posterior, −3.7 mm; medial/lateral, 3 mm; dorsal/ventral, −4.8 mm; 0° angle; targeting ventral subciulum). Two days after viral infusion, the animals underwent an accelerated defeat protocol in which they were subjected to social defeat stress two times daily for 10 minutes over four days.

Sdk1 viral surgery for neurophysiological recordings

We developed the "cannutrode" system to infuse virus into previously implanted animals and thereby quantify the effect of VHip-Sdk1 overexpression using a within-subject design. For *in vivo* recording experiments, animals were implanted with recording electrodes as specified above. A cannula

was built into the microwire bundle targeting left VHip. Additionally, a 360um diameter cannula (MicroLumen, Oldsman, FL) was implanted above right VHip, Both of the cannulas were implanted to a depth of 1mm. After the initial forced interaction test experiment, mice were anesthetized with 1.5% isoflurane, and a 33-gauge Hamilton syringe was used to bilaterally infuse 0.5 µl HSV vector at a rate of 0.1 µl/min through the cannula into VHip.

This cannutrode system was critical for using HSV viruses to interrogate the impact of molecular pathways on *Electome* activity, since our mice required 10-14 days to recover from electrode implantation, and HSV transgene expression is limited to 1-5 days after infection.

Viral Histology

Animals were perfused with 4% paraformaldehyde and brains were harvested and stored for 24 hours in PFA. Brains were cryoprotected with sucrose and frozen in OCT compound and stored at -80C. Brains were sliced at 35µm and stained using anti-GFP (ThermoFisher, Waltham, MA) and Alexa488-anti-rabbit (ThermoFisher, Waltham, MA) antibodies using standard methods. Images were obtained using a Nikon Eclipse fluorescence microscope at 4x and 10x magnifications.

IFNα dosing

We utilized an IFNα administration protocol that has been previously shown to induce depression-like behavior in mice[17]. Briefly, mice were injected with either mouse IFNα ($4x10^5$IU/kg i.p; Miltenyi Biotec, Auburn, CA) diluted in phosphate-buffered saline (PBS) or a PBS vehicle for 5 weeks. Implanted animals were tested in the sucrose preference test and forced interaction test. Non-implanted animals were tested in the social interaction test and open field. Animals continued to receive daily injections throughout the course of the study.

Maternal Separation and Social Defeat Stress

Maternal separation was performed as described previously[18]. Briefly, the experimental pups were separated from their dams for three hours each day on post-natal days (PNDs) 1-14, and control pups were reared under standard conditions. During the separation period, the pups were placed on a heating pad and remained in contact with their littermates. Animals were weaned on day 21.

For behavioral experiments, males were subjected to SDS starting when they were eight-ten weeks old (or were left as controls). The SDS paradigm was performed as described previously[19] and consisted of introducing each experimental mouse into the home cage of a singly housed resident CD1 male for five minutes a day for ten days. The experimental mice were introduced into the home cage of a new CD1 male mouse each day. On day 11, experimental animals were tested for social avoidance behavior or were sacrificed for molecular analyses. For *in vivo* physiology experiments, animals were implanted at 14-16 weeks, and the forced interaction test was performed after a 2 week recovery period.

SSFO Experiments

Mice were anesthetized with 1.5% isoflurane and placed in a stereotaxic device. A 33-gauge Hamilton syringe was used to infuse 0.5 µl of AAV2-CaMKIIa-SSFO-EYFP vector at a rate of 0.1 µl/min into left IL_Cx (1.7mm AP, 0.25mm ML, 2mm DV from the dura). An AAV2-Ef1a-DIO-SSFO-EYFP vector was used a non-expressing control. Two weeks later, mice were anesthetized again, and recording electrodes will implanted as described above. A fiberoptic cannula was built into the IL_Cx/PrL_Cx bundle[2, 20]. The tip of the fiberoptic was situated 250µm above the tip of the IL recording microwires (i.e., targeting the dorsal IL_Cx border). *In vivo* recordings were conducted after a 2 week recovery. SSFO expression was confirmed histologically in IL_Cx in 6 out of the 8 animals. Five of the six SSFO mice

showed a strong suppression of IL_Cx gamma activity immediately following blue light stimulation. None of the DIO-SSFO mice exhibited this physiological response, thus the one SSFO mouse that did not demonstrate IL_Cx gamma suppression was removed from subsequent analysis in the IL_Cx-DBS study.

Ketamine Experiments

Mice used for SSFO experiments were used for ketamine experiments after a 1 week "washout" period to return to baseline. Mice were pseudorandomized to the ketamine or saline group such that half of the mice in each group were infected with SSFO, and the other half were infected with DIO-SSFO. This pseudo randomization was performed in order to avoid any confounds that may have resulted from prior IL_Cx-DBS. Mice were injected with ketamine (20mg/kg, i.p.) twenty-four hours prior to the forced interaction test. Critically, while prophylactic administration of ketamine (20mg/kg, i.p.) has been shown to prevent the subsequent emergence of behavioral dysfunction in 129S6/SvEv strain mice subjected to cSDS[21], this ketamine administration strategy is not effective is preventing stress induced behavioral dysfunction in C57 mice[21, 22]. Ketamine (Ketathesia®, Henry Schein, 100mg/mL) was diluted in saline to a concentration of 5mg/mL prior to administration.

Statistical Justification

Table 1: Statistical Analyses

Experiment	Comparison	Statistical Test	Tails
Unbiased testing Pre-Stress *Electome*	Susceptible vs. Resilient	Wilcoxon rank-sum Receiver Operating Characteristic AUC	Two-Tailed
Unbiased testing Neuron-*Electome*	Cells and *Electome* Correlation	Spearman Regression with Shuffling	'Two-Tailed'
Validation testing of sdk1 impact on susceptibility	Sdk1 vs. Control	Wilcoxon rank-sum	One-Tailed
Validation Pre-Stress *Electome*	Sdk1 vs. Control	Wilcoxon rank-sum	One-Tailed
Unbiased testing of sdk1 effect on social behavior	Sdk1 vs. Control	Two-way ANOVA (Group)	Two-Tailed
Unbiased testing of sdk1 effect on forced swim	Sdk1 vs. Control	T-test	Two-Tailed
Validation Social Deficit	IFNa vs. Control	Mixed Model ANOVA (Group Effect) Post-hoc unpaired t-test (Social Time)	One-Tailed
Unbiased testing to establish Sucrose Pref. Assay	Sucrose vs. Water	Paired t-test	Two-Tailed
Validation Sucrose Pref. Deficit	IFNa vs. Control	Mixed Model ANOVA (Sucrose Effect) Post-hoc paired t-test (Within group)	One-Tailed
Validation Pre-Stress *Electome*	IFNa vs. Control	Wilcoxon rank-sum	One-Tailed
Unbiased testing to establish Vulnerability in ELS model	ELS vs. Subthreshold cSDS	Two-way ANOVA (Interaction) Post-hoc t-test (within, across groups)	Two-Tailed
Validation Pre-Stress *Electome*	ELS vs. Control	Wilcoxon rank-sum	One-Tailed
Validation Pre-stress *Electome 1*	IL-DBS vs. Sham	Wilcoxon rank-sum	One-Tailed
Validation Pre-stress *Electome 2 and 3*	IL-DBS vs. Sham	Mixed Model ANOVA (Group Effect) w/ Box-Cox Transformation Post-hoc Wilcoxon rank-sum	One-Tailed
Validation Pre-Stress *Electome 1*	Ketamine vs. Saline	Wilcoxon rank-sum	One-Tailed
Validation Pre-Stress *Electome 2 and 3*	Ketamine vs. Saline	Mixed Model ANOVA (Interaction Effect) w/ Box-Cox Transformation Post-hoc Wilcoxon rank-sum	One-Tailed

We used multiple-kernel machine learning to define behaviorally relevant *Electomes*. Post-hoc testing was not performed on the across-group differences observed post-stress since this was a learned feature of our CSFA model. The stress-susceptibility/resilience identities of animals was not utilized to supervise training of the pre-stress neural data. Thus, pre-stress differences in *Electome* activity could be quantified. This was accomplished using a two-tailed Wilcoxon rank-sum test at $\alpha=0.05$. We did not correct for multiple comparisons in this analysis since our chosen strategy was to validate all of the

significant *Electome* differences using complete out-of-sample testing. Our *a priori* hypothesis for this subsequent validation testing was that other depression vulnerability models would show the same *Electome* differences identified in the vulnerable mice prior to cSDS. All out-of-sample testing to validate *Electome 1* and *Electome 2* as signatures of stress-vulnerability (sdk1, IFNα, and ELS) was performed using a one-tailed Wilcoxon rank-sum test. Using this one-tailed testing strategy allowed us to constrain the number of animals needed per group while retaining statistical power. Finally, we combined the p-values for the three independent validations sets using a Fisher's combined probability test. With this approach, we were able to increase the number of independent validation paradigms (5 total independent validation experiments for the study, with 6-8 animals per manipulation or control group for each experiment).

For testing aimed at validating depression-related behavior in the previously published sdk1 and IFNα models (i.e. three chamber social interaction), statistical analyses were performed using one-tailed tests. For the sucrose preference experiment, we first established the paradigm in an independent cohort of C57 mice (see supplemental Figure S1). We then tested our *a priori* hypothesis that mice chronically treated with IFNα would show a disruption in sucrose preference compared to mice treated with vehicle. This was achieved with one-tailed ANOVA. For testing establishing depression-related behavior in the ELS-vulnerability model for which there was no prior literature, statistical analysis was performed using a two-tailed test.

Our *a priori hypothesis* for the anti-depressant manipulation validation studies was that anti-depressive therapeutics (IL-DBS or ketamine) would fail to suppress *Electome 1* activity. We used a one-tailed Wilcoxon rank-sum test for this analysis. We also tested the effect of these manipulations on *Electome 2* and *3* activity. Since *Electome 2* and *3* activity was increased in the mice that exhibited depression-like behavioral dysfunction after cSDS, our *a priori* hypothesis for this analysis was that the anti-depressant manipulations would suppress activity in these *Electomes*. We used a one-tailed mixed-model-ANOVA for this analysis. Post-hoc testing was performed with a one-tailed Wilcoxon rank-sum test. Again, using this one-tailed testing strategy allowed us to constrain the number of animals needed per group while retaining statistical power.

Detailed Author Contributions

RH performed *in vivo* recording and behavioral experiments for chronic social defeat stress; performed sdk1 *in vivo* recording study; jointly conceived the early life stress study; performed early life stress *in vivo* recording study; performed histological analysis; wrote the paper.
KU conceived and developed the CSFA statistical approach; analyzed LFP data for chronic social defeat stress experiment; wrote the paper.
BDS jointly conceived the early life stress experiments; performed early life stress behavioral experiment and analyzed data; performed the early life stress *in vivo* recording experiment.
CB jointly developed the sucrose preference assay; built recording electrodes for IL_Cx-DBS, ketamine, sdk1 and IFNα study; assisted with IL_Cx-DBS physiology experiment; performed behavioral experiments for IFNα study; analyzed the behavioral data for IFNα study; assisted with IFNα physiology experiment; performed histological analysis.
DEC performed all of the *Electome* transformation analyses for the IL_Cx-DBS, ketamine, sdk1, IFNα, and ELS *in vivo* recording experiments; wrote the paper.
NN assisted with IL_Cx-DBS physiology experiment; performed behavioral experiments for IFNα study; analyzed the behavioral data for IFNα study; assisted with IFNα physiology experiment; performed histological analysis.

RB jointly conceived the sdk1 experiment, performed sdk1 behavioral experiments and analyzed data; wrote the paper.
EP performed sdk1 behavioral experiments and analyzed data.
MTV jointly developed the sucrose preference assay.
JW jointly developed the cannutrode *in vivo* recording approach, built electrodes for sdk1 experiments.
AJS jointly conceived the IFNα experiments, wrote the paper.
KDe jointly conceived the IL_Cx-DBS experiments, provided viral reagents, wrote the paper.
SDM performed *in vivo* recording experiments for IL_Cx-DBS study, jointly developed the sucrose preference assay, performed *in vivo* recording experiments for IFNα study, supervised behavioral experiments for IFNα study; performed histological analysis.
MGC supervised behavior experiments for early life stress study.
EJN jointly conceived chronic social defeat stress and sdk1 experiments; provided viral reagents, supervised sdk1 behavioral experiments; wrote the paper.
LC supervised the development of CSFA model; supervised analysis of *in vivo* recording data for chronic social defeat stress, sdk1, IFNα, and ELS experiments; wrote the paper.
KDz conceived the Ketamine experiment, and jointly conceived the chronic social defeat stress, SSFO, sdk1 and IFNα experiments; jointly conceived and designed cannutrode system, performed ketamine, IL_Cx-DBS, sdk1, and IFNα *in vivo* recording experiments and analyzed data; conceived and performed cellular firing analysis; supervised all aspects of chronic social defeat stress, sdk1, and IFNα studies; supervised in vivo recording experiments for early life stress study; wrote the paper.

Supplemental References

1. Bagot, R.C., et al., *Circuit-wide Transcriptional Profiling Reveals Brain Region-Specific Gene Networks Regulating Depression Susceptibility.* Neuron, 2016. **90**(5): p. 969-83.
2. Hultman, R., et al., *Dysregulation of Prefrontal Cortex-Mediated Slow-Evolving Limbic Dynamics Drives Stress-Induced Emotional Pathology.* Neuron, 2016. **91**(2): p. 439-52.
3. Kumar, S., et al., *Prefrontal cortex reactivity underlies trait vulnerability to chronic social defeat stress.* Nat Commun, 2014. **5**: p. 4537.
4. Berton, O., et al., *Essential role of BDNF in the mesolimbic dopamine pathway in social defeat stress.* Science, 2006. **311**(5762): p. 864-8.
5. Krishnan, V., et al., *Molecular adaptations underlying susceptibility and resistance to social defeat in brain reward regions.* Cell, 2007. **131**(2): p. 391-404.
6. Golden, S.A., et al., *A standardized protocol for repeated social defeat stress in mice.* Nat Protoc, 2011. **6**(8): p. 1183-91.
7. Ulrich, K., et al., *GP Kernels for Cross-Spectrum Analysis.* Advances in Neural Information Processing Systems, 2015. **28**.
8. Gönen, M. and E. Alpaydın, *Multiple Kernel Learning Algorithms.* Journal of Machine Learning Research, 2011. **12**: p. 2211-2268.
9. Titsias, M.K. and M. Lazaro-Gredilla. *Spike and slab variational inference for multi-task and multiple kernel learning*. in *NIPS*. 2011.
10. A., Á.M., L. Rosasco, and N.D. Lawrence, *Kernels for vector-valued functions: a review. .* Foundations and Trends in Machine Learning, 2011: p. 195-266.
11. Rasmussen, C.E. and C.K.I. Williams, *Gaussian Processes for Machine Learning*. 2006: the MIT Press.
12. Wilson, A. and R. Adams, *Gaussian Process Kernels for Pattern Discovery and Extrapolation.* Proc. Int. Conf. Machine Learning, 2013.

13. Zhu, J., A. Ahmed, and E.P. Xing. *MedLDA: maximum margin supervised topic models for regression and classification*. in *ICML*. 2009.
14. Cortes, C. and V. Vapnik, *Support-vector networks.* Machine Learning, 1995: p. 273-297.
15. Mairal, J., et al., *Online learning for matrix factorization and sparse coding.* Journal of Machine Learning Research 2010. **11**: p. 19-60.
16. Pu, Y., et al. *A deep generative deconvolutional image model*. in *AISTATS*. 2015.
17. Zheng, L.S., et al., *Mechanisms for interferon-alpha-induced depression and neural stem cell dysfunction.* Stem Cell Reports, 2014. **3**(1): p. 73-84.
18. Sachs, B.D., et al., *The effects of brain serotonin deficiency on behavioural disinhibition and anxiety-like behaviour following mild early life stress.* The international journal of neuropsychopharmacology, 2013: p. 1-14.
19. Sachs, B.D., J.R. Ni, and M.G. Caron, *Brain 5-HT deficiency increases stress vulnerability and impairs antidepressant responses following psychosocial stress.* Proceedings of the National Academy of Sciences of the United States of America, 2015.
20. Kumar, S., et al., *Cortical Control of Affective Networks.* J Neurosci, 2013. **33**(3): p. 1116 –1129.
21. Brachman, R.A., et al., *Ketamine as a Prophylactic Against Stress-Induced Depressive-like Behavior.* Biol Psychiatry, 2016. **79**(9): p. 776-86.
22. Donahue, R.J., et al., *Effects of striatal DeltaFosB overexpression and ketamine on social defeat stress-induced anhedonia in mice.* Biol Psychiatry, 2014. **76**(7): p. 550-8.